

DISKLIKE STRUCTURE IN THE SEMIREGULAR PULSATING STAR X HERCULIS

JUN-ICHI NAKASHIMA¹

Received 2004 August 26; accepted 2004 October 31

ABSTRACT

This paper reports the results of a Berkeley-Illinois-Maryland (BIMA) array interferometric observation of a semiregular pulsating star with an unusual narrow molecular line profile, X Her, in the CO $J = 1-0$ line. In the CO spectrum, a double-component profile (including narrow and broad components) is seen, as reported by previous observations. The narrow component consists of two spiky peaks. The spatial structure of the broad component shows bipolar shape, and that of the narrow component shows an elliptical/spherical shape. The two peaks in the narrow component show a systematic difference in the integrated intensity map. The kinematical and geometrical properties of the narrow component are reminiscent of a Keplerian rotating disk with a central mass of $0.9 M_{\odot}$, although an interpretation as an expansion disk seems to be more natural. A secondary bipolar flow instead of the disk also cannot be fully excluded as an interpretation of the narrow line.

Subject headings: circumstellar matter — stars: AGB and post-AGB — stars: imaging — stars: individual (X Herculis) — stars: late-type — stars: mass loss

1. INTRODUCTION

A nonnegligible number of asymptotic giant branch (AGB)/post-AGB stars are known to show peculiar molecular line profiles that exhibit unusual small line widths. The width of the peculiar narrow line is often less than 5 km s^{-1} . Such a narrow-line profile is difficult to explain as an AGB wind with a typical expansion velocity of about 10 km s^{-1} . Among CO profiles of AGB stars, peculiar narrow-line profiles are known in 5%–10% of the sample (see, e.g., Winters et al. 2003). The narrow line was first found toward AGB stars with double-component line profiles (Knapp et al. 1998; Kerschbaum & Olofsson 1999); in these envelopes, the narrow and broad lines have the same central velocity. The narrow lines have so far been found in several types of AGB stars. Knapp et al. (1998) have reported the narrow lines toward both M- and C-type AGB stars. Kerschbaum & Olofsson (1999) also have found the narrow lines toward four semiregular pulsating AGB stars. Kahane & Jura (1996) have found similar narrow lines toward chemically peculiar AGB stars, BM Gem and EU And; these stars are known as “silicate carbon stars,” which simultaneously have a C-rich central star and O-rich circumstellar material. Nakashima & Deguchi (2004) have recently reported a detection of the narrow line toward an unusual SiO maser source with a rich set of molecular species, IRAS 19312+1950, and they have suggested that this object is also an AGB/post-AGB star, although the evolutionary status of this object is not definitely known yet. AGB stars with only the narrow component (without the broad component) have also been found (Kerschbaum & Olofsson 1999; Winters et al. 2003), but these are chemically normal. To explain the origin of the double-component profile including the narrow line, Knapp et al. (1998) have advanced a hypothesis that takes multiple shell winds into account, in which each shell has different expanding velocities produced by episodic mass loss with highly varying gas expansion velocities. In addition, Kahane & Jura (1996) have suggested that the narrow lines seen in the silicate carbon stars could be explained by gravitationally stable material in the form of a distorted or puffed-up slowly rotating

disk, in which O-rich material is trapped. Interestingly, Bergman et al. (2000) have reported a tentative detection of a Keplerian disk toward an O-rich AGB star with the narrow line, RV Boo.

To investigate the properties of peculiar narrow lines in AGB stars, high-resolution interferometric observations were made with the Berkeley-Illinois-Maryland Association (BIMA) array toward a sample of AGB stars exhibiting narrow molecular line profiles. This paper reports the first result of interferometric observations in the CO $J = 1-0$ line toward a semiregular pulsating star with normal O-rich chemistry, X Her, and shows an indication of disk structure around the central star. X Her (IRC +50248; SAO 45863; IRAS 16011+4722) is a semiregular pulsating AGB star that has the typical narrow line; this star was reported in the General Catalog of Variable Stars (Kholopov et al. 1985) to have a period of 95 days. There also exists a second period of 746 days (Houk 1963). The double-component profile of X Her was found first by Kahane & Jura (1996), and they also provided the first spatial information on X Her through their single-dish mapping observation. Kahane & Jura (1996) found that the broad symmetric line of X Her consists of a bipolar flow, and that the overall spatial structure of the narrow line is almost spherical. The annual parallax of this star (7.26 mas with 1σ uncertainty of 0.70 mas) was measured by the *Hipparcos* satellite, giving the distance of $126\text{--}152 \text{ pc}$. In this paper the distance of 138 pc is adopted.

2. OBSERVATION AND RESULTS

Interferometric observations of X Her were made with the BIMA array from 2004 February to May. The instrument has been described in detail by Welch et al. (1996). The author observed the CO $J = 1-0$ line at 115.271202 GHz with the BIMA array, consisting of 10 elements in 4 configurations (A, B, C, and D). The observations were interleaved every 25 (for the B, C, and D arrays) or 10 minutes (for the A-array) with the nearby point sources, 3C 345 and 1613+342, to track the phase variations over time. The absolute flux calibration was determined from observations of Uranus and MWC 349, and is accurate to within 20%. The final map has an accumulated on-source observing time of about 31 hr. Typical single-sideband system temperature ranges from 250 to 500 K. The velocity

¹ Department of Astronomy, University of Illinois at Urbana-Champaign, 1002 West Green Street, Urbana, IL 61801; junichi@astro.uiuc.edu.

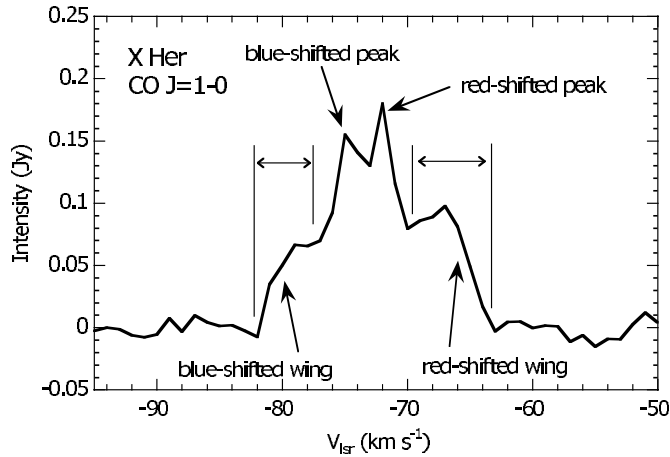


FIG. 1.—Spatially integrated spectrum of X Her in the CO $J = 1-0$ line. The integrated area is a circle with a diameter of $15''$. The vertical solid lines represent the velocity ranges of the blue- and redshifted wings. Each kinematical component is indicated by the arrows.

coverage is about 350 km s^{-1} , using three different correlator windows with a bandwidth of 50 MHz each. The velocity resolution is 1.03 km s^{-1} . The phase center of the map is R.A. = $16^{\text{h}}02^{\text{m}}39^{\text{s}}.1739$, decl. = $47^{\circ}14'25''.279$ (J2000.0). Data reduction was performed with the MIRIAD software package (Sault et al. 1995). Standard data reduction, calibration, imaging, and deconvolution procedures were followed. Robust weighting of the visibility data gives a $3''.11 \times 2''.48$ CLEAN beam with a position angle of $37''.18$. The rms noise per 1.0 km s^{-1} is $3.71 \times 10^{-2} \text{ Jy beam}^{-1}$.

Figure 1 shows the spatially integrated spectrum of the CO $J = 1-0$ line. In the spectrum two kinematical components are seen, as reported by Kahane & Jura (1996): the “broad wing component” (V_{LSR} range -82 to -63 km s^{-1}) and “narrow component” (V_{LSR} range -76 to -70 km s^{-1}). Furthermore, the narrow component consists of two kinematical components, the “blueshifted peak” ($V_{\text{peak}} \sim -75 \text{ km s}^{-1}$) and the “redshifted peak” ($V_{\text{peak}} \sim -72 \text{ km s}^{-1}$). These kinematical components are indicated by the arrows in Figure 1. The continuum radiation is not detected at the 3σ rms level, although the frequency channels were integrated over 150 MHz using the opposite sideband to the line observation of CO. The upper limit of the flux of the continuum radiation at the 3 mm band (center frequency $\sim 112 \text{ GHz}$) is $6.2 \times 10^{-3} \text{ Jy}$. To investigate the spatial distribution of each kinematical component, velocity-integrated intensity maps were made; the maps are shown in Figure 2. The structure seen in Figure 2 is clearly resolved by our synthesized beam. According to the peak intensity of the CO spectrum ($0.18 \text{ Jy beam}^{-1}$), about 5% of the flux detected by the IRAM 30 m telescope (Kahane & Jura 1996) was detected in the present interferometric observation. As reported by Kahane & Jura (1996), in the upper panel of Figure 2 we can clearly see the bipolar shape consisting of the blue- and redshifted wings of the broad component (*thin and thick contours*), and also the spherical shape consisting of the narrow component (*gray broken contours*). The angular size of the bipolar shape (above 5σ level) is $12''.4$ (length) and $11''.8$ (width); this angular size corresponds to a linear size of $2.6 \times 10^{16} \text{ cm}$ (length) and $2.4 \times 10^{16} \text{ cm}$ (width) at a distance of 138 pc. Strictly speaking, according to our high-resolution map, the spatial structure of the narrow component seems to be elliptical rather than spherical (this is more remarkable in the lower panel of Fig. 2; see below). The best result of fitting by elliptic curves to the 5σ

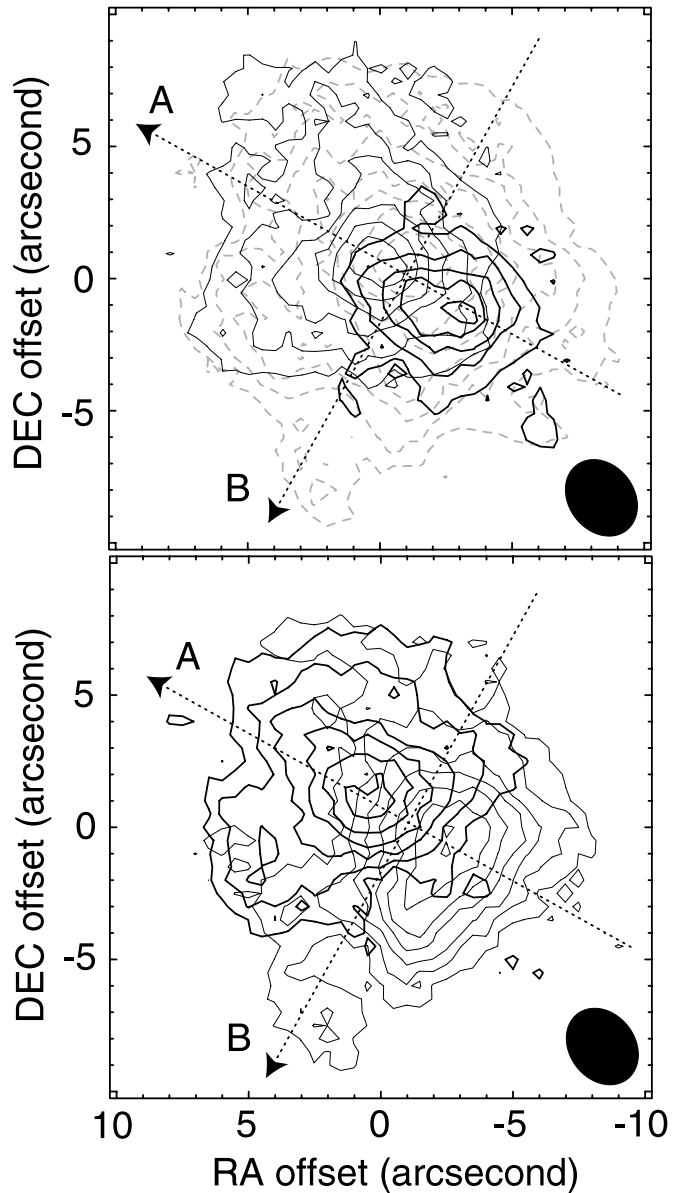


FIG. 2.—Velocity-integrated intensity maps of the kinematical components indicated in Fig. 1. In the upper panel, the thick and thin contours represent the maps of the blue- and redshifted wings, respectively; the gray broken contours represent the map of combined intensity of the blue- and redshifted peaks. In the lower panel, the thick and thin contours represent maps of the blue- and redshifted peaks, respectively. The dotted arrows represent the cuts used for Fig. 3. The synthesized beam size is indicated in the lower right corners. The contours start from a 5σ level, and the increment of the contours are every 2σ . In the upper panel the 1σ levels for the thick, thin, and broken contours are 1.516×10^{-2} , 1.238×10^{-2} , and $1.403 \times 10^{-2} \text{ Jy beam}^{-1}$, respectively. In the lower panel, the 1σ level is $2.144 \times 10^{-2} \text{ Jy beam}^{-1}$ for both the thick and thin contours. The velocity integration ranges for the wings are -82 to -77 (blue-shifted wing) and -71 to -63 (redshifted wing), and those of the red- and blueshifted peaks are 3 km s^{-1} each (the peak velocities are taken at the center of the range).

level contour, which is expected to be undisturbed by an effect of the beam pattern, gives the angular sizes of major and minor axes of the elliptical shape, $15''.1$ and $12''.6$, respectively; these angular sizes correspond to linear sizes of $3.1 \times 10^{16} \text{ cm}$ (major axis) and $2.6 \times 10^{16} \text{ cm}$ (minor axis) at the distance of 138 pc.

The lower panel of Figure 2 shows velocity-integrated intensity maps of the blue- and redshifted peaks. Interestingly, in the lower panel of Figure 2 we can clearly see a systematic

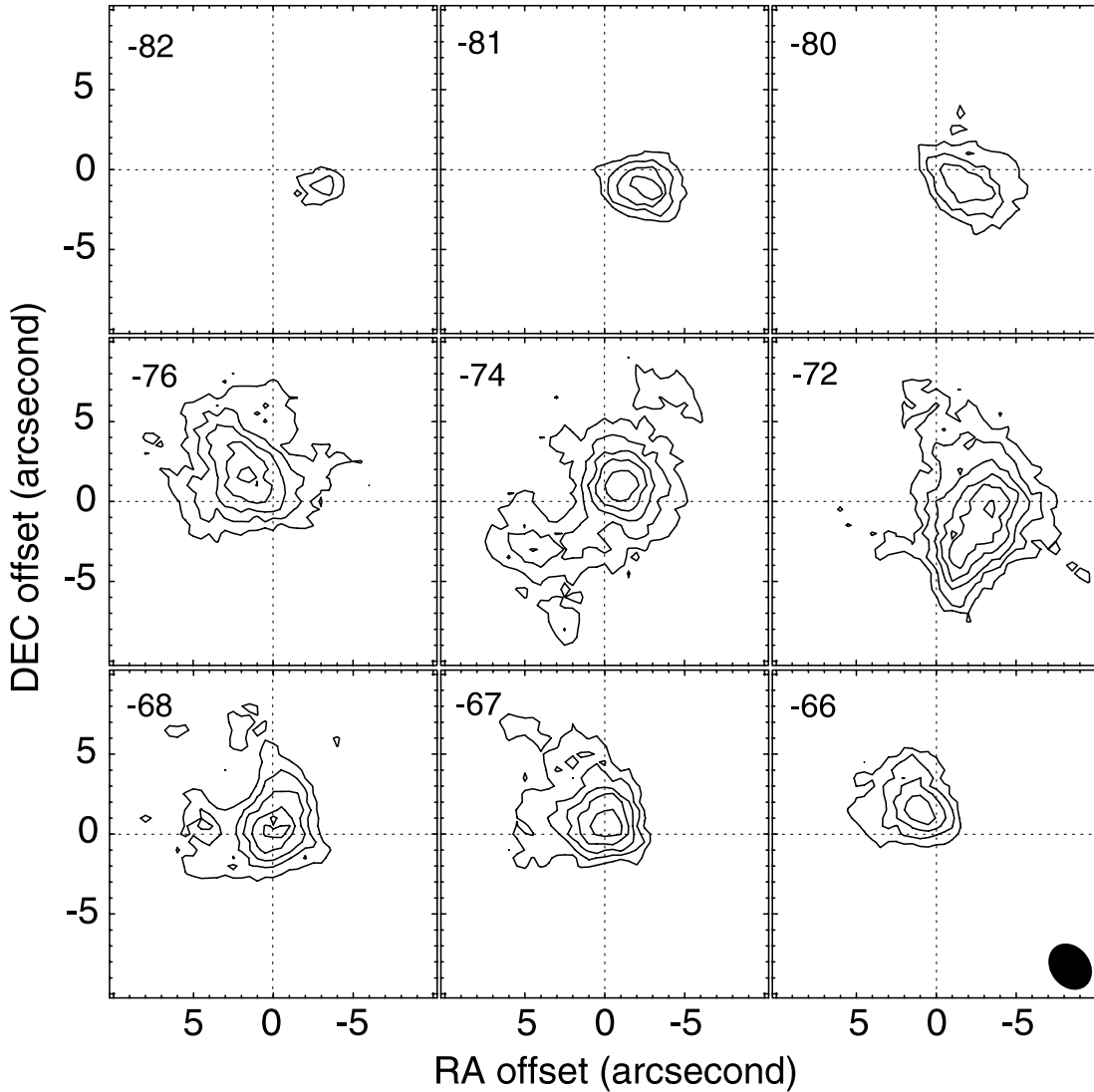


FIG. 3.—Selected channel maps of the CO $J = 1-0$ line. The channel velocities are indicated in the upper left corner of each panel. The velocity channels were averaged over 2 km s^{-1} intervals. The contours start from 5σ level, and the increment of the contours is every 2σ . The 1σ level corresponds to $2.63 \times 10^{-2} \text{ Jy beam}^{-1}$. The synthesized beam size is indicated in the lower right corner.

difference between the shapes of the thin and thick contours. This phenomenon is also confirmed in velocity channel maps; the maps are shown in Figure 3. In Figure 3 the top, middle, and bottom panels correspond to the blueshifted wing, the narrow component, and the redshifted wing, respectively. The channel maps clearly show that the CO source structure varies with velocity. The velocity structure of the narrow component seen in Figure 3 (*middle panels*) seems to be varying systematically, while the variation of the structure at the higher velocity ranges seen in the top (-82 to -80 km s^{-1}) and bottom (-68 to -66 km s^{-1}) panels seems to originate in the bipolar flow reported by Kahane & Jura (1996).

3. DISCUSSION

To precisely investigate the kinematical properties of the narrow component, position–velocity (p - v) diagrams were made in various cuts with various position angles. Figure 4 shows two selected p - v diagrams. The origin of the cuts are taken at the apparent symmetric center of the spatial structure of the narrow component: $(\Delta \text{R.A.}, \Delta \text{decl.}) = (1''0, 0''1)$. The cuts used in Figure 4 are indicated by the dotted arrows in Figure 2. The

most remarkable velocity structure has been found in the position angle 61° (cut A); on the other hand, the velocity structure almost totally disappears in the position angle 151° (cut B), which is perpendicular to cut A. In the upper panel of Figure 4, we can clearly see a systematic variation of structure as a function of the radial velocity. Although the velocity structure originating in the bipolar flow seems to contaminate to the data, especially in higher velocity ranges, the structure of the narrow component is symmetrically placed in velocity with respect to the line center ($V_{\text{sys}} \sim 73.5 \text{ km s}^{-1}$). This kinematical structure is reminiscent of Keplerian rotation (see, e.g., Fig. 8 in Ohashi et al. 1997). The structure can actually be fitted well by a Keplerian rotation curve with the central mass of $0.9 M_\odot$ at the distance of 138 pc; this Keplerian rotation curve is superimposed on the upper panel of Figure 4. The central mass calculated by the Keplerian fitting is to the point as a mass of the star of this type if we rely on edge on view. If the elliptical shape seen in Figure 2 represents the true geometry of the disk, we can crudely estimate the orbital inclination angle of the Keplerian disk on the assumption of thin-disk geometry. In such a case, with the length of the major and minor axes gave in the previous

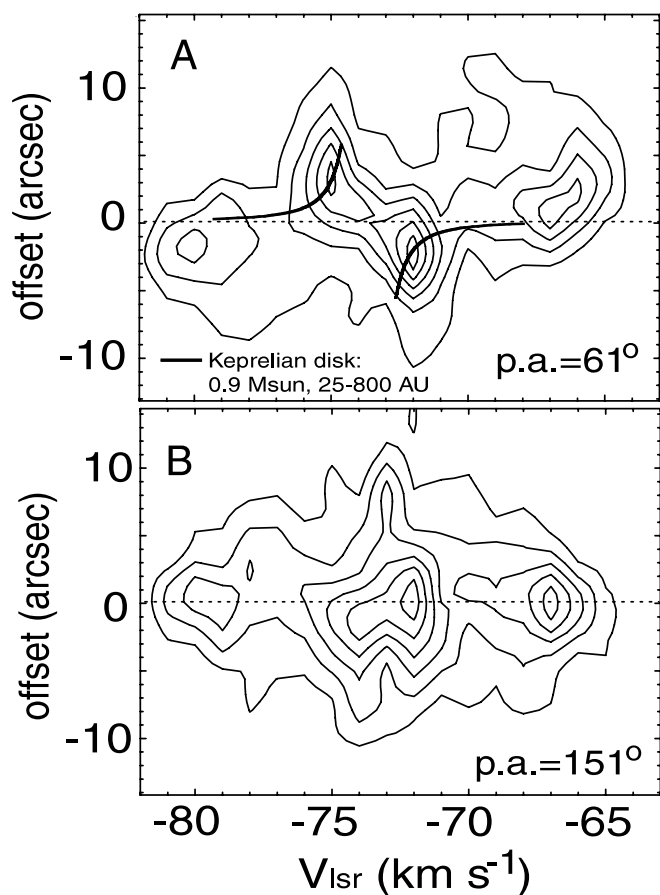


FIG. 4.—Position-velocity diagrams for the cuts indicated in Fig. 2. The contour levels correspond to 90%, 75%, 60%, 45%, 30%, and 15% of the intensity peak. The names of the cuts and the position angles are indicated in the upper left and lower right corners of each panel, respectively. The solid curve indicated in the upper panel represents the best-fit result of the Keplerian disk to the data (see text). The broken horizontal lines represent the origin of the offset axes.

section, the orbital inclination angle of the Keplerian disk is calculated to be 57° ; this angle leads to the corrected central mass of $3.0 M_\odot$. This corrected mass seems to be somewhat heavier than that expected for X Her, because the luminosity of AGB stars, in general, varies as a function of a main-sequence mass of the star, and also because the luminosity of X Her is typical for an AGB star with a main-sequence mass of about $1 M_\odot$ (Vassiliadis & Wood 1993). In fact, the total luminosity of X Her is estimated to be about $9200 L_\odot$ from V and I_C -band fluxes (Platais et al. 2003), J , H , K , L' , and M -band fluxes (Kerschbaum & Hron 1994), and the IRAS 12 and $25 \mu\text{m}$ fluxes on the basis of a linear interpolation (Deguchi et al. 2002). Therefore, if the narrow component really originates in a Keplerian rotating disk, in my opinion, an interpretation along the lines of a geometrically thick disk, which is observed in closely edge-on view, is tempting. One problem remaining in the Keplerian disk interpretation is the physical/geometrical relationship between the bipolar flow and the disk. If the axes of the bipolar flow and the Keplerian disk correspond, the kinematical properties seen in the present results are rather difficult to explain unless we assume existence of outflow (or expansion) in the disk. In fact, a simple expanding disk model suggested by Hirano et al. (2004) seems to on some level explain the integrated intensity maps shown in Figure 2 (compare Fig. 4 in Hirano et al. 2004), although the velocity scale of their model is totally different

from the present case. The geometrical correspondence of axes between bipolar flow and disks has frequently been required in recent AGB/post-AGB studies to explain the formation of the bipolar flows seen in AGB/post-AGB stars. If the expansion disk is the case, there remains no indication of Keplerian rotation.

A secondary bipolar flow instead of expansion of the disk might be an alternative explanation for the narrow component. However, in such a case, the very slow expansion velocity ($\sim 1.5 \text{ km s}^{-1}$) is problematic unless it is a projection effect, because recent studies suggest that the bipolar flow of AGB/post-AGB stars originates in an AGB wind, and also because in such a case the velocity of the bipolar flow is expected to be at least typical of an AGB wind ($10\text{--}20 \text{ km s}^{-1}$) or higher. If the slow expansion velocity originates in the projection effect, the inclination angle of the secondary bipolar flow is estimated to be about 81° , on the assumption that the expansion velocity of the secondary bipolar flow is equivalent to a half of the full line width of the broad component ($\sim 10 \text{ km s}^{-1}$). In such a large inclination, the elliptical shape (which is almost spherical) is unlikely to be explained by the bipolar flow if the true structure of the bipolar flow is well collimated. However, we must note that, in terms of dynamical age, the secondary bipolar flow may be produced within the duration of the AGB phase in the evolution of X Her, because the dynamical timescale of the secondary bipolar flow is estimated to be 6500 yr; the order of this value is equivalent to the value calculated by Kahane & Jura (1996). Thus, at the moment, the possibility of the secondary bipolar flow cannot be fully excluded. We should note that Kerschbaum et al. (2003) have recently presented an SiO ($v = 0, J = 1\text{--}0$) map taken by the Very Large Array (VLA); the map also suggests a Keplerian rotating disk around X Her, but in a direction orthogonal to the disk in this paper, although the data of Kerschbaum et al. (2003) are of marginal quality. To draw a more firm conclusion about this question, higher resolution and higher sensitivity data are required.

Although several AGB stars with narrow lines exhibit chemical peculiarity, no evidence of such peculiarity has been found so far in X Her. González Delgado et al. (2003) have detected both the broad and narrow kinematical components toward X Her in the thermal millimeter line of the SiO molecule. They have estimated the column density of SiO, but have found no peculiarity in SiO abundance; it is fairly normal for an O-rich AGB star. The *IRAS* LRS class of X Her is 24; this also suggests that X Her is a normal O-rich star with emission feature of silicate. As a possible interpretation of this normality of the chemical condition of X Her, the author suggests that the kinematical properties of the (possible) disk is critical for the chemistry of the star. The key is the duration of material in the disk; this duration is constrained by the kinematical properties of the disk. Thus, if the expansion is dominant in the disk, the disk cannot effectively trap material for a long time; conversely, if the Keplerian rotation is dominant, the disk may effectively trap plenty of material for a relatively long time. Therefore, if the chemical environment of the star changes during the duration, the star may have complex (or multiple) chemical environments, such as the C/O-rich mixture seen in silicate-carbon stars. This mechanism was first discussed by Jura & Kahane (1999). According the present results, the disk of X Her seems to include expanding motion (although other possibilities cannot be excluded). Therefore, the material included in the disk of X Her is limited to that expelled recently. To confirm this hypothesis, it is hoped that AGB/post-AGB stars with the narrow line and chemical peculiarities, such as

silicate carbon stars, will be observed by high-resolution radio interferometry, so that the results can be compared with those of chemically normal AGB stars with the narrow line, such as X Her. Generally speaking, the intensities of the narrow lines seen in AGB stars are very weak, and is difficult to observe them with current equipments, but next-generation interferometers will enable us to increase the number of observations of AGB stars with narrow lines.

4. SUMMARY

In this paper, the author reports a result of an interferometric observation of the semiregular pulsating AGB star, X Her, in the CO $J = 1-0$ line. In the CO spectrum, a double-component profile, including narrow and broad components, is seen, as

reported by Kahane & Jura (1996). The narrow component consists of two peaks; these peaks shows a systematic difference in the integrated intensity map. The kinematical properties of the narrow component is reminiscent of a Keplerian disk with a central mass of $0.9 M_{\odot}$, although the possibilities of a bipolar flow and expanding disk instead of Keplerian motion cannot be excluded.

This research has been supported by the Laboratory for Astronomical Imaging at the University of Illinois and by NSF grant AST 02-28953, and has made use of the SIMBAD and ADS databases.

REFERENCES

- Bergman, P., Kerschbaum, F., & Olofsson, H. 2000, *A&A*, 353, 257
 Deguchi, S., Fujii, T., Nakashima, J., & Wood, P. R. 2002, *PASJ*, 54, 719
 González Delgado, D., Olofsson, H., Kerschbaum, F., Schoier, F. L., Lindqvist, M., & Groenewegen, A. T. 2003, *A&A*, 411, 123
 Hirano, N., et al. 2004, *ApJ*, 616, L43
 Houk, N. 1963, *AJ*, 68, 253
 Jura, M., & Kahane, C. 1999, *ApJ*, 521, 302
 Kahane, C., & Jura, M. 1996, *A&A*, 310, 952
 Kerschbaum, F., & Hron, J. 1994, *A&AS*, 106, 397
 Kerschbaum, F., & Olofsson, H. 1999, *A&AS*, 138, 299
 Kerschbaum, F., et al. 2003, *Rev. Mod. Astron.*, 16, 171
 Kholopov, P. N., et al. 1985, *General Catalog of Variable Stars* (4th Ed.; Moscow: Moscow Publishing House)
 Knapp, G. R., Young, K., Lee, E., & Jorissen, A. 1998, *ApJS*, 117, 209
 Nakashima, J., & Deguchi, S. 2004, *ApJ*, 610, L41
 Ohashi, N., Hayashi, M., Ho, P. T. P., & Momose, M. 1997, *ApJ*, 475, 211
 Platais, I., et al. 2003, *A&A*, 397, 997
 Sault, R. J., Teuben, P. J., & Wright, M. C. H. 1995, in *ASP Conf. Ser. 77, Astronomical Data Analysis Software and Systems IV*, ed. R. A. Shaw, H. E. Payne, & J. J. E. Hayes (San Francisco: ASP), 433
 Vassiliadis, E., & Wood, P. R. 1993, *ApJ*, 413, 641
 Welch, W. J., et al. 1996, *PASP*, 108, 93
 Winters, J. M., Le Bertre, T., Jeong, K. S., Nyman, L.-Å., & Epchtein, N. 2003, *A&A*, 409, 715